ACS APPLIED MATERIALS & INTERFACES

Research Article

www.acsami.org

Adhesion and Proliferation of Human Mesenchymal Stem Cells from Dental Pulp on Porous Silicon Scaffolds

Pierre-Yves Collart-Dutilleul,[†] Emilie Secret,[‡] Ivan Panayotov,[†] Dominique Deville de Périère,[†] Raúl J. Martín-Palma,[§] Vicente Torres-Costa,[§] Marta Martin,[⊥,∥] Csilla Gergely,[⊥,∥] Jean-Olivier Durand,[‡] Frédérique Cunin,[‡] and Frédéric J. Cuisinier*[,†]

[†]BioNano Laboratory EA 4203, Montpellier 1 University, Montpellier, France

[‡]Institut Charles Gerhardt Montpellier, UMR-5253 CNRS-UM2-ENSCM-UM1, Ecole Nationale Supérieure de Chimie de Montpellier, 34296 Montpellier, France

[§]Departamento de Física Aplicada, Universidad Autónoma de Madrid, 28049 Cantoblanco, Madrid, Spain

[⊥]Université Montpellier 2, UMR 5221 Laboratoire Charles Coulomb, Montpellier, France

[∥]CNRS, Laboratoire Charles Coulomb UMR 5221, Montpellier, France

Supporting Information

ABSTRACT: In regenerative medicine, stem-cell-based therapy often requires a scaffold to deliver cells and/or growth factors to the injured site. Porous silicon (pSi) is a promising biomaterial for tissue engineering as it is both nontoxic and bioresorbable. Moreover, surface modification can offer control over the degradation rate of pSi and can also promote cell adhesion. Dental pulp stem cells (DPSC) are pluripotent mesenchymal stem cells found within the teeth and constitute a readily source of stem cells. Thus, coupling the good proliferation and differentiation capacities of DPSC with the textural and chemical properties of the pSi substrates provides an interesting approach for therapeutic use. In this study, the behavior of human DPSC is analyzed on pSi substrates presenting pores of various sizes, 10 ± 2 nm, 36 ± 4 nm, and 1.0 ± 0.1 μm, and undergoing different chemical treatments, thermal oxidation, silanization with aminopropyltriethoxysilane (APTES), and hydrosilylation with undecenoic acid or semicarbazide. DPSC adhesion and proliferation were followed for up to 72 h by fluorescence microscopy, scanning electron microscopy (SEM), enzymatic activity assay, and BrdU assay for mitotic activity. Porous silicon with 36 nm pore size was found to offer the best adhesion and the fastest growth rate for DPSC compared to pSi comporting smaller pore size (10 nm) or larger pore size (1 μm), especially after silanization with APTES. Hydrosilylation with semicarbazide favored cell adhesion and proliferation, especially mitosis after cell adhesion, but such chemical modification has been found to led to a scaffold that is stable for only 24−48 h in culture medium. Thus, semicarbazide-treated pSi appeared to be an appropriate scaffold for stem cell adhesion and immediate in vivo transplantation, whereas APTES-treated pSi was found to be more suitable for long-term in vitro culture, for stem cell proliferation and differentiation.

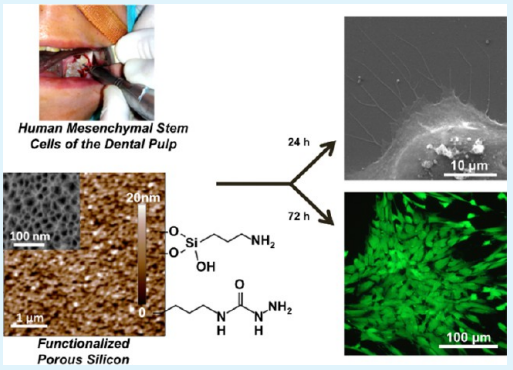

KEYWORDS: *porous silicon, dental pulp stem cells, cell adhesion, surface functionalization, tissue engineering*

INTRODUCTION

In regenerative medicine, tissue engineering applications are based on the development of biological substitutes that can restore, maintain or even improve tissue functions: tissue engineering combines cells and bioactive factors in a defined microenvironment created by a biomaterial scaffold. A key component for tissue engineering is the biomaterial scaffold that, ideally, should support cell attachment, proliferation and differentiation, and be biocompatible and biodegradable at a controlled rate.[1] Stem-cell-based therapy often requires a scaffold to carry cells to the injured site. Porous silicon (pSi) appears to be a promising biomaterial for tissue engineering as it is both nontoxic and bioresorbable under physiological conditions and dissolves progressively into nontoxic silicic acid.[2] Its dissolution rate is dependent on the pore geometry and surface chemical properties, and these two factors influence cell adhesion.[3,4] Moreover, this tunable, biocompatible, and resorbable material has been reported to favor the growth of hydroxyapatite, suggesting the possible bone implantability of the material.[5] Its biocompatibility and immunogenicity has already been demonstrated under different conditions and it additionally offers useful photoluminescence properties.[6]

Received: October 21, 2013
Accepted: January 16, 2014
Published: January 16, 2014

dx.doi.org/10.1021/am4046316 | ACS Appl. Mater. Interfaces 2014, 6, 1719−1728

Furthermore, pSi-based scaffolds have been investigated for orthopedic[7] and ophthalmic implants,[8] for controlling the adhesion and proliferation of different cell types,[3,9,10] and even as intravenously injectable particles for imaging tumors in vivo[11] or retina pressure actuators.[12]

Surface treatment resulting in accessible porosity with chemically stable inner surface is a key step to prevent rapid hydrolysis and degradation of the porous matrix in aqueous cell culture environments, without eliciting any undesirable effects on the cells. Moreover, surface chemical modification by turning pSi from hydrophobic to hydrophilic promotes cell adhesion and growth.[3,13] The most common and simple surface treatment is oxidation, which can be performed by either ozone, aging, thermal, or chemical treatments. Amine-terminated modifications as silanization with aminopropyl trimethoxysilane or triethoxysilane improve pSi chemical stability and enhance cell adhesion in comparison to oxidized pSi.[3] Thermal hydrosilylation was also used to graft chemical species to generate a substrate for cell adhesion and proliferation, such as dodecene, undecenoic acid, or oligoethylene glycol.[9]

Substrate topography has been known for a long time to affect crucial cell functions, namely adhesion, proliferation, migration, and differentiation. Moreover, material surface morphology has strong effects on cell cytoskeleton and morphology.[14] Furthermore, cellular organization requires that a cell assess its relative location, taking in multiple cues from its microenvironment, i.e., the extracellular matrix in vivo, and the supporting scaffold in vitro.[15] Cells respond to topographic surfaces in a wide variety of ways, which depend upon cell type, pore size, as well as the physicochemical properties of the substrate material. The effect of pore size and porosity of pSi on cell growth is of particular relevance. Indeed, its pore dimensions can be precisely controlled and are highly tunable during pSi electrochemical anodization. A variety of pore sizes can be produced: from micropores (< 2 nm), mesopores (2−50 nm) to macropores (> 50 nm) depending on the preparation conditions.[16] Although microscale topography modulates cellular behaviour in vitro, it is important to consider that cells in vivo make contact with microscale as well as nanoscale topographical features. Diverse topographical features have been assessed for different cell types, at the micrometer and submicrometer scale, and some recent studies on pSi have focused specifically on pore geometry influence on cell adhesion and proliferation.[17−20] Pore geometry was clearly shown to affect the cellular response, but each cell type responded differently. Rat hippocampal neurons were observed to preferentially adhere on macroporous surfaces, with a pore size ranging between 50 and 100 nm, rather than on flat silicon surfaces.[17] Neuroblastoma cells cultured over continuous porous gradient substrates were more likely to develop on surface topography with feature sizes of <20 nm, and substrates with an average pore size of a few hundreds of nanometers restricted cell adhesion and proliferation.[4] Primary human endothelial cells, mouse fibroblasts, mouse neuroblastoma cells, and human cortical neuron cell lines adhered and proliferated more on mesoporous silicon than on flat silicon, with a tendency to proliferate more on pSi with an average pore size of ∼5 nm, rather than ∼20 nm.[20] It is of interest to note that this was, so far, the only study assessing primary human cells. Rat mesenchymal stem cells (rMSC) adhesion was enhanced as pore size decreased, with a maximum proliferation for an average pore size of ∼20 nm but responded more strongly to surface chemical changes during short-term culture[19] and had a high proliferation rate also on flat silicon.[18]

Coupling the auspicious capacities of human adult mesenchymal stem cells (hMSC) with the unique properties of pSi substrates provides a promising approach for therapeutic application in regenerative medicine. Indeed, mesenchymal stem cells therapeutic potential has generated significant excitement in the field of regenerative medicine, as they can be found in various niches within human body. The ability of these cells to self-renew and differentiate into multiple tissues makes them an attractive cell source for cell-based regenerative therapies. MSCs have considerable potential for the treatment of musculoskeletal disorders because of their expansion capacity, immunosuppressive properties, and ability to differentiate into bone and cartilage.[21] Adult stem cells constitute the source of differentiated cells for the regeneration of tissues that are diseased or injured. In adults, these cells are accessible from different origins, such as bone marrow, adipose tissue, or dental pulp.[22]

In this study, we investigated for the first time the behavior of primary culture of hMSC on pSi scaffolds. Mesenchymal stem cells from the dental pulp, named human dental pulp stem cells (DPSC),[23] were studied for adhesion and proliferation on oxidized mesoporous and macroporous pSi substrates, presenting pore size of 10 ± 2 nm, 36 ± 4 nm, and 1.0 ± 0.1 μm. We also evaluated the influence of pSi substrate surface modification with CO_2H, NH_2, or $NHCONHNH_2$ groups on the cell behavior. After characterization of the silicon substrates, cell adhesion and proliferation behavior were studied using fluorescence and electron microscopy, enzymatic proliferation assays and bromodeoxyuridine (BrdU) incorporation for the detection of proliferating cells.

MATERIALS AND METHODS

Human Dental Pulp Stem Cells (DPSC). Human impacted third molar extracted for orthodontic reasons were recovered from healthy patients (15−18 years of age). Written informed consent was obtained from the parents of the patients. This protocol was approved by the local ethical committee (Comité de Protection des Personnes, Montpellier hospital, France). Tooth surfaces were cleaned using 2% chlorhexidine and cut around the cementum−enamel junction by using sterilized disc. The teeth were then broken into two pieces to reveal the pulp chamber. The pulp tissue was gently separated from the crown and root and then digested in a solution of 3 mg/mL collagenase type I and 4 mg/mL dispase (BD Biosciences, Bedford, MA) for 1 h at 37 °C. The solution was then filtered through 70 μm Falcon strainers and immersed in αMEM supplemented with 10% fetal bovine serum (FBS), 100 U/mL penicillin, 100 μg/mL streptomycin (all from Invitrogen, Carlsbad, CA, USA) and placed in 75 mL flasks. Cells were incubated for 1 week at 37 °C with 5% CO_2. Nonadherent cells were removed by a change of medium 24 h after cell seeding.

DPSC Characterization. After 1 week, subconfluent cells were collected and analyzed for minimal criteria to define human mesenchymal stem cells, such as adherence to plastic, expression of cell surface antigens and ability to differentiate into osteoblasts, adipocytes and chondroblasts in vitro.[24] The antigen profiles of cultured DPSCs were analyzed by detecting the expression of the cell surface markers CD90, CD146, CD117, and CD45 using flow cytometry (all antibodies from Miltenyi Biotec, Paris, France).[25,26] Cells were controlled for

pluripotency with in vitro osteogenic, adipogenic and chondrogenic differentiation following a previously described protocol.[27]

Porous Silicon (pSi) Scaffold Preparation. Silicon wafers were obtained from Siltronix (Siltronix, Archamps, France). P++ type boron-doped crystalline silicon wafers with 0.0008 - 0.0012 Ωcm resistivity were obtained from Siltronix. Wafers were etched in a custom-made Teflon cell at a constant current density of either 30 mA/cm^2 for 10 min or 300 mA/cm^2 for 2 min 15 s, in a hydrofluoric acid (HF) solution in ethanol (3:1 HF:ethanol solution, volume ratio). To create pSi with larger pores (1 μm), p-type ⟨100⟩ wafers with 7 - 21 Ωcm resistivity were etched at a constant current density of 4.5 mA/cm2 for 10 min, in a 50% HF solution in dimethylformamide (DMF, Sigma, St Louis, MO, USA). Etched wafers were oxidized at 800°C for 1 h. The wafers were cut into 0.5 cm^2 pieces. Some of the samples etched in a 300 mA/cm^2 current were also submitted to various chemical treatments: silanization with aminopropyltriethoxysilane (APTES) after thermal oxidation (as described above), hydrosilylation with undecenoic acid without pre-oxidation treatment, and hydrosilylation with semicarbazide without pre-oxidation treatment (all reagents from Sigma, St Louis, MO, USA). PSi surface modifications with APTES, and with undecenoic acid were described elsewhere.[3,9] The covalent attachment of the semicarbazide to hydrogen-terminated pSi surfaces by thermal hydrosilylation was realized according to recently published procedure using tert-butyl-2[(allylamino)carbonyl]hydrazine carboxylate.[28] The removal of the protecting group yields a semicarbazide-terminated monolayer.[29] For use in cell culture, the wafers were sterilized with 70% ethanol (volume ratio) for 10 min before drying under sterile airflow.

Surface Characterization. The topography of the surface modified pSi samples was analyzed by environmental scanning electron microscopy (SEM) (Analytic FEI Quanta FEG 200) to determine the pore size, and by atomic force microscopy (AFM) (Asylum MFP-3D, Asylum Research, Santa Barbara, CA) to determine the surface roughness. SEM images were treated and analyzed using imageJ® software to measure the mean diameter of the pores visible at the surface. For SEM, an acceleration voltage of 20.00 kV was used in a pressure of 0.5 Torr. For AFM, gold-coated silicon nitride rectangular cantilevers were used with a typical spring constant of 30 pN/nm^{-1}, tip radius ∼30 nm (BL-RC150 VB-C1: Bio-Lever A, Olympus Optical Co., Ltd., Tokyo, Japan). The spring constant for each cantilever was determined by thermal noise method within the supplied software. Height images were recorded in tapping mode in liquid at room temperature. Typically, 512 × 512 point scans were taken at a scan rate of 1 Hz per line.

Surface tension was determined using sessile drop contact angle measurements, conducted in a custom-made set-up consisting of a syringe dispenser, a sample stage, a macro lens and a CCD camera. Five microliters of Milli-Q water was spotted onto the surface at room temperature. Images of the drop profiles were captured and ImageJ software was used to measure contact angles on both sides of the droplet. A minimum of four replications was conducted for each sample surface.

Cell Adhesion. DPSC attachment was monitored by fluorescence microscopy. Cells were seeded onto the surface of sterilized pSi at a cell density of 5 × 10^4 cell/mL. Flat silicon (non etched silicon wafers) and glass coverslip were used as controls. Cells were incubated for 4, 24, 48, and 72 h at 37 °C with 5% CO_2, in a humidified incubator, in ultra low adherence 24-well plates (Corning, NY, USA) that inhibit cell attachment on the tissue culture plate, allowing DPSC to attach only to the pSi. After the incubation time, the cells were fixed with 2.5% glutaraldehyde and stained with 50 μg/mL of 4,6-diamidino-2-phenylindole (DAPI, Sigma, St Louis, MO, USA) for 30 min before being washed with phosphate buffer saline (PBS; Invitrogen, Carlsbad, CA, USA) to remove any non-adherent cells. Cells were observed under fluorescence microscopy at an excitation wavelength of 290 nm. Controls were cells cultured on glass coverslip and flat silicon, cut into 0.5 cm^2 squares. Cell counts were conducted at five different locations on the surface of each sample (four peripheral and one central) in areas of 1400 μm × 1050 μm. the number of viable cells for each experimental condition was counted and represented on a linear graph. The doubling time (DT) was determined from the growth curves and by using the formula

$$\mathrm{DT} = (t - t_0)\log 2/(\log N - \log N_0)$$

where t and t_0 were the times at which the cells were counted, and N and N_0 were the cell numbers at times t and t_0, respectively.[30]

Proliferation Assays. Cell proliferation was first measured via quantification of acid phosphatase activity using para-nitrophenylphosphate phosphatase test (pNPP).[31] By assessing acid phosphatase activity, we considered the physiological activity of the attached cells. Indeed, after adhesion, cells require restarting their physiological activity and pNPP assay has been shown to be simple, sensitive and convenient to detect lysosomal enzyme activity.[32] DPSC proliferation was assessed after 4, 24, 48, and 72 h incubation. At the end of each experimental time, the cells were washed three times with PBS and lysed with 500 mL of the acid phosphatase lysis buffer (0.1 M sodium acetate, 0.1% Triton X-100, pH 5.5), supplemented with 1 mg/mL of pNPP (all products from Sigma, St Louis, MO, USA). After 1 h incubation at 37 °C, the reaction was stopped by the addition of 10 μL of 1 N NaOH (Sigma, St Louis, MO, USA). The supernatant was removed and placed in a new 24-well plate and the yellow colorimetric reaction was measured by a microtiter plate reader at 405 nm. All proliferation experiments were performed at least in triplicate and results were normalized according to the glass coverslip control at 72 h, for which 100% of proliferation was attributed.

The proliferation rate of DPSCs on pSi was also assessed by bromodeoxyuridine (BrdU, Invitrogen, Carlsbad, CA, USA) incorporation for 24 h.[33] DPSC were seeded on the various pSi scaffolds at a density of 10^5 cells/ml in αMEM supplemented with 10% FBS with 1:100 diluted BrdU labeling (Invitrogen, Carlsbad, CA, USA). After 24 h incubation at 37°C, samples were rinsed 3 times in PBS, fixed in 4% paraformaldehyde, rinsed again 3 times in PBS and put in 1.5M HCl (Sigma, St Louis, MO, USA) for 30 min at room temperature to dissociate DNA strands. Samples were washed with PBS, incubated in PBS with 0.1% Triton X-100 and 1% BSA for 1 h at room temperature, then incubated with mouse anti-BrdU primary antibody (Milteny) overnight at 4 °C. After immunostaining, cells were washed with PBS/1% BSA, incubated with FITC conjugated rabbit anti-mouse secondary antibody for 30 min and counterstained with 2μg/mL Hoeschst 33342 (Sigma, St Louis, MO, USA) for nucleus staining. Samples were observed under fluorescence microscopy at an excitation wavelength of 290 nm for nuclei (blue staining) and 490 nm for BrdU (green staining). All experiments were performed at least in triplicate

and the number of BrdU-positive cells was expressed as a percentage of the total number of cells, counted at five different points per sample.

Cellular Morphology and Viability. Fluorescein diacetate (FDA) and propidium iodide (PI) staining was used to observe cell morphology and to distinguish viable and dead cells (both products from Invitrogen, Carlsbad, CA, USA). FDA, which enters viable cells by energy-dependent endocytosis, yield a bright green color; while PI, which interacts with RNA and DNA of cells having disrupted cytoplasmic and nuclear membranes, produces a red color.[34] Living cells were stained with 25 μg/mL of fluorescein diacetate (FDA) and 20 μg/mL of propidium iodide (PI), and incubated for 3 min at 37°C. After staining, samples were washed with PBS before being observed under a Nikon TE2000-E microscope equipped with a Nikon digital camera at an excitation wavelengths of 480 nm for FDA and 630 nm for PI. Observations were conducted at five different locations on the surface of each sample (four peripheral and one central) at magnifications ×20 and ×40. All experiments were made in triplicate.

SEM Evaluation of DPSC Morphology and Spreading. The cells were cultured on the various pSi scaffolds and control for 24 h under normal conditions, as described above. After 24 h incubation the cells were washed twice with PBS buffer and fixed with 2.5% glutaraldehyde for 1 h at room temperature. After washing the specimens were dehydrated in graded ethanol solutions from 50% to 100%, and in hexamethyldisilazane (HMDS, Ted Pella, Redding, CA, USA). The samples were then sputter-coated with platinum. Scanning electron microscopy (SEM) was performed on an Analytic FEI Quanta FEG 200 microscope with an acceleration voltage of 15 kV in a pressure of 1×10^{-5} Torr. From the SEM images, two parameters for characterizing the cell morphology were considered: the cell area (in μm^2), defined as the area covered by the cell projected over the substrate and the cell circularity, defined as the ratio between the shorter and the longer axis of the cell (value between 0 for elongated cells and 1.00 for round cells). All experiments were made in triplicate.

Statistical Analysis. All data were evaluated with a Shapiro-Wilk normality test. The cell attachment evaluations (cell counts) were plotted as mean ± standard error of the mean and statistical analyses were performed using a parametric Student t-test. The results of proliferation experiments with pNPP enzymatic assays were normalized according to the glass coverslip control at 72 h, for which 100% of proliferation was attributed. The data were plotted as mean ± standard error of the mean and statistical analyses were performed using a parametric Student t-test. The results of BrdU proliferation assay, cell surface area and cell circularity were analyzed with a non-parametric one-way Tukey ANOVA test (SigmaStats, SPSS Inc., Chicago, IL, USA). A p-value of <0.05 was considered to be significant.

RESULTS

pSi Samples. PSi substrates were generated from bulk boron-doped p-type silicon wafers via anodization.[16] Substrates with various pore sizes were obtained by modulating the etching conditions and the doping level of the silicon wafer. Figure 1 shows representative SEM and AFM images of the pSi substrates; distinct textural features are depicted when comparing the different pSi substrates.

PSi substrates obtained from silicon wafers with a resistivity of 0.0008−0.0012 Ω cm by applying a constant current density

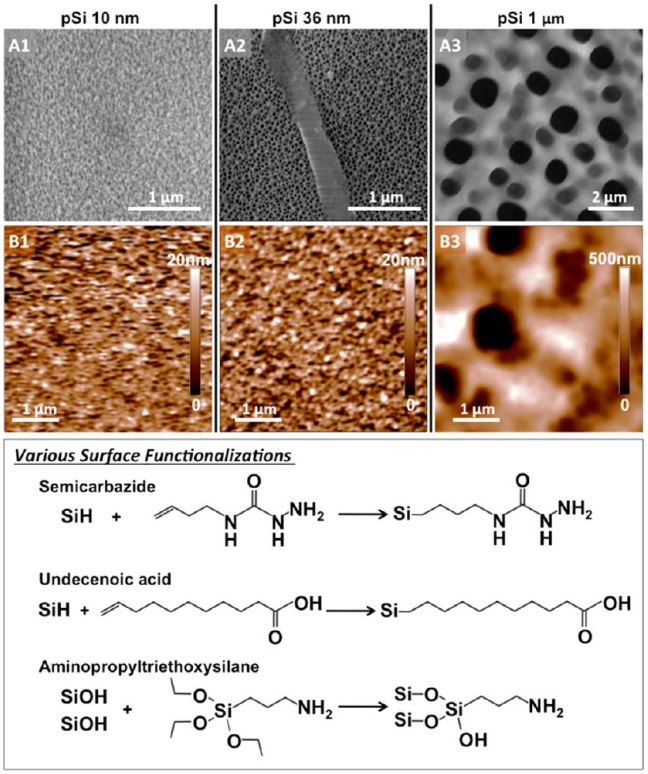

Figure 1. Characterization of the porous silicon scaffolds. Surface topography of the silicon substrates imaged with (A) scanning electron microscopy and (B) atomic force microscopy. Porous silicon with mean pore diameter of 10, 36, and 1 μm are shown as A1-B1, A2-B2, and A3-B3, respectively. Schemas of surface chemical treatments are presented as: nonoxidized pSi hydrosililation with semicarbazide; nonoxidized pSi hydrosililation with undecenoic acid; oxidized pSi silanization with APTES.

of 30 mA/cm^2 and 300 mA/cm^2 had an average pore diameter of 10 ± 2 nm (pSi 10 nm) and 36 ± 4 nm (pSi 36 nm), respectively. The pSi layers produced from silicon wafers with 7−21 Ω cm resistivity, by applying a current density of 4.5 mA/cm^2, had an average pore diameter of 1020 ±100 nm (pSi 1 μm). The pSi substrates were quite uniformly porosified. Topographic images of pSi were obtained using AFM, and the calculated root-mean-squared roughness (R_{rms}) of the substrate were found at 1.9 ± 0.7 nm for "pSi 10 nm", 7 ± 2 nm for "pSi 36 nm", and 54 ± 20 nm for "pSi 1 μm". R_{rms} is given by the standard deviation of the z-values (surface heights) for the sample area, as given by equation

$$R_{rms} = \sqrt{\sum_{n=1}^{N} \frac{(Zn - \overline{Z})^2}{N}}$$

where N is the number of points in the image of the surface.

Although experimental determination of the surface roughness is almost always conducted using AFM, there is some difficulty is comparing our results to those reported in the literature because of variation in the methods applied and the sample areas examined.

Surface chemical treatments realized on "pSi 36 nm" substrates are hydrosilylation with undecenoic acid or semicarbazide, and silanization (after thermal oxidation) with APTES. The reaction schemes of the chemical treatments are presented in Figure 1. The sample pSi 36 nm was chosen

because it displayed the best results in term of cell adhesion, compared to pSi 10 nm and pSi 1 μm (Figure 2). Water contact

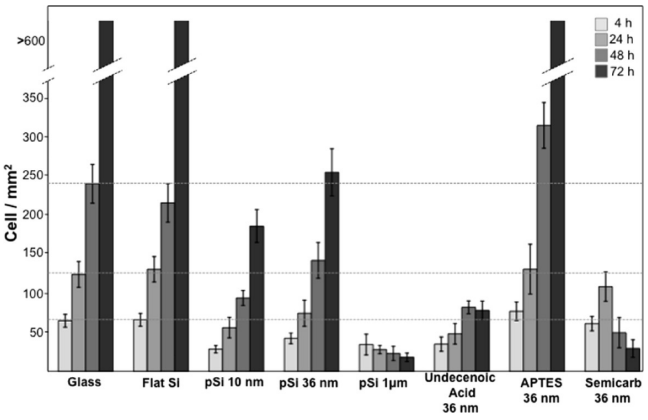

Figure 2. DPSC attached on various type of pSi, after 4, 24, 48, and 72 h of incubation (left columns to right columns, respectively). Glass coverslip and flat silicon were used as control. Cells were counted per surface measuring 1400 μm × 1050 μm, in five areas per samples. Mean values are expressed as cell numbers per mm^2, with error bars corresponding to standard deviation. The bars protruding from the frame correspond to cells reaching confluence.

angle measurements performed after surface functionalization revealed that all the substrates were hydrophilic (Table 1). All

Table 1. Water Contact Angle of the Various Scaffolds (flat Si and pSi)

	water contact angle (deg)			
	flat Si	pSi 10 nm	pSi 36 nm	pSi 1 μm
oxidized	26 ± 4	16 ± 2	15 ± 3	33 ± 5
undecenoic acid			35 ± 5	
APTES			37 ± 6	
semicarbazide			12 ± 3	

the modified surfaces were hydrophilic in agreement with the data of the literature: freshly etched pSi surfaces without oxidation are highly hydrophobic with contact angles of 108–130°.[29,35–38] Thermal oxidation increases wettability.[36,38] Oxidized pSi hydrophilicity was attributed to the removal of Si_ySiH_x species from the surface and to the formation of a polar Si–OH capped surface after oxidation.[39] After oxidation or hydrosilylation the values drop from 12 to 37° showing the successful functionalization of the surfaces with hydrophilic groups. By analyzing SEM micrographs, the surface porosities (ratio between total area of the pores and the area of the considered region of interest) were found to be as follows: 40 ± 4% for pSi 10 nm, 45 ± 6% for pSi 36 nm, and 24 ± 4% for pSi 1μm.

Cell Adhesion and Growth. We examined DPSC attachment to various surface-modified pSi layers and compared the results with those of DPSCs cultured on glass coverslips and on flat silicon wafers after a period of 4, 24, 48, and 72 h. The results are shown in Figure 2.

The experimental results showed that initial cell adhesion and growth were very similar on glass coverslip, Flat Si, APTES-treated pSi and semicarbazide-treated pSi, after 4 h and 24 h. Initial cell adhesion on oxidized pSi (pSi 10 nm, pSi 36 nm and pSi 1μm) and undecenoic acid-treated pSi were significantly lower compared to glass coverslip ($p < 0.001$, $p = 0.003$, $p < 0.001$, and $p < 0.001$, respectively). However, DPSC started to proliferate on pSi 10 nm and pSi 36 nm after 24 h following the same growth pattern observed on glass coverslip, whereas the number of cells slightly decreased on pSi 1 μm and on undecenoic acid-treated pSi after 24 and 48 h, respectively. After 48 h, the numbers of cells were similar on glass coverslip and on flat Si, significantly higher on APTES-treated pSi ($p<0.001$) and significantly lower on semicarbazide-treated pSi ($p < 0.001$), pSi 10 nm ($p < 0.001$), and pSi 36 nm ($p < 0.001$). It is remarkable that there were significantly more cells on pSi 36 nm than on pSi 10 nm after 48 and 72 h ($p = 0.006$ and $p = 0.004$, respectively), and that the number of cells on semicarbazide-treated pSi increased during 24 h and decreased abruptly after 48 h. After 72 h, DPSC reached confluence on glass coverslip, flat Si, and APTES-treated pSi. Cells exhibited a mean doubling time of approximately 27, 30, 33, and 28 h on glass coverslip, flat Si, pSi 10 nm, and pSi 36 nm, respectively. On functionalized scaffolds (hydrosilylated or silanized 36 nm

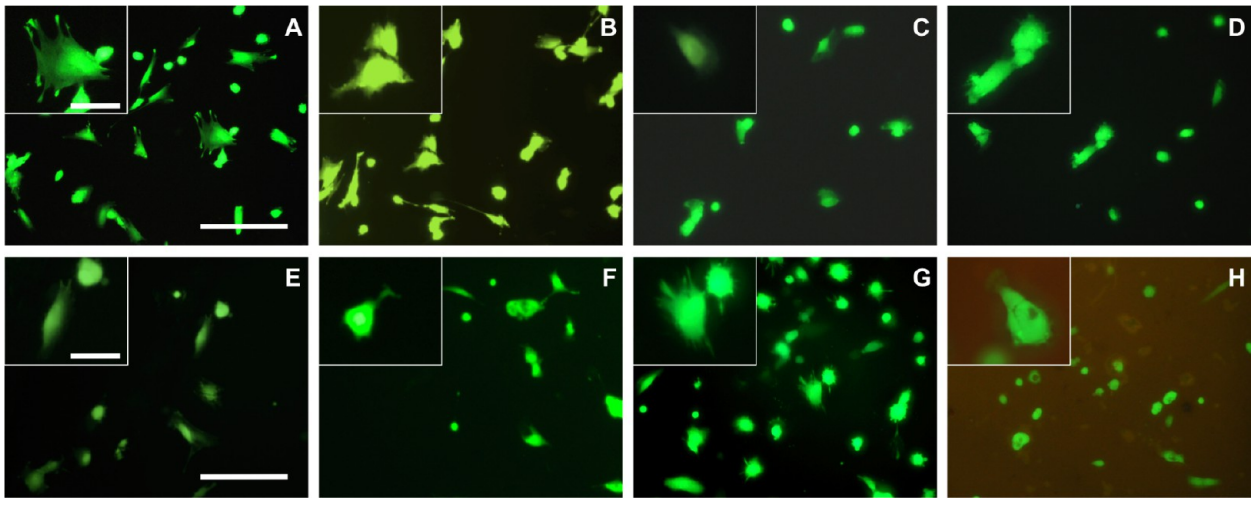

Figure 3. Fluorescence microscopy of DPSC on various pSi scaffolds after 4 h incubation. Cells are stained with vital FDA staining (cytoplasma: green staining). (A) glass coverslip, (B) flat Si, (C) pSi 10 nm, (D) pSi 36 nm, (E) pSi 1μm, (F) undecenoic acid-treated 36 nm pSi, (G) APTES-treated 36 nm pSi, (H) semicarbazide-treated 36 nm pSi. Main pictures: ×20, bar = 100 μm. Insets: magnification ×40, bar = 40 μm.

dx.doi.org/10.1021/am4046316 | ACS Appl. Mater. Interfaces 2014, 6, 1719–1728

pSi) cells showed a mean doubling time of 24 h on APTES-treated and semicarbazide-treated pSi. It was not possible to measure or calculate doubling time on pSi 1 μm and undecenoic-acid-treated pSi.

Cells were stained with the vital dye FDA to observe cell adherence and cytoplasmic spreading. The morphologies of DPSC on surface-modified pSi at early attachment stage (after 4 h) are shown in Figure 3.

From Figure 3, it is obvious that cells attached on all surfaces, with various shapes from normal fibroblastic morphology (Figure 3A, B, and G) to less-spread cells with protrusions (Figure 3C, D), and even round cells (Figure 3E, F, and H). Fibroblastic morphologies were found mainly on glass coverslip, flat Si and APTES-treated pSi. Cells with protrusions were mainly found on pSi 10 nm and pSi 36 nm, whereas round cells with few protrusions were recovered on pSi 1 μm, undecenoic-acid-treated pSi and semicarbazide-treated pSi. These results correlate well with the results on cell adhesion described from Figure 2.

Cell Proliferation. DPSC proliferation over a 3-day-time period, assessed by acid phosphatase activity, was evaluated for the various pSi scaffolds, and compared to that of glass coverslip and Flat Si. To normalize the results, we attributed 100% cell enzymatic activity to the value found for glass coverslip after 72 h of cell incubation (Figure 4).

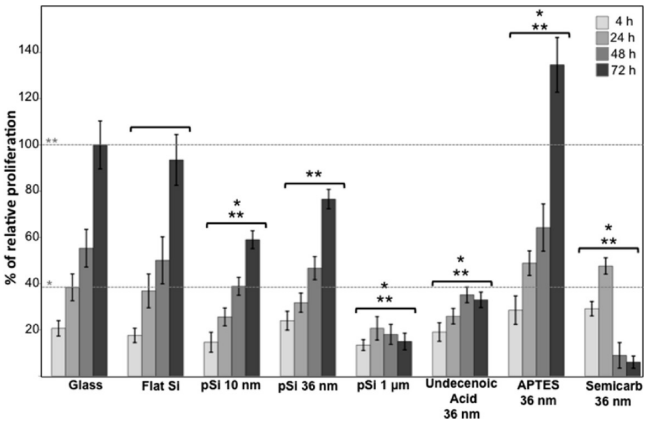

Figure 4. DPSC proliferation at 4, 24, 48, and 72 h on various pSi surfaces, assessed by acid phosphatase activity determination. Glass coverslip and oxidized non-porous silicon (flat Si) were used as control. To normalize the results, 100% adhesion was attributed to cells attached on glass coverslip after 72 h of cell seeding. All experiments were performed in triplicate. Statistical significance was determined by using the Student's t test ($P < 0.05$) for comparison with glass coverslip: (*) statistical difference at 24 h, (**) statistical difference at 72 h.

The experiments showed that DPSCs clearly proliferated at all time points on glass coverslip, flat Si, pSi 10 nm, pSi 36 nm, and APTES-treated pSi, whereas the proliferation was limited on pSi 1 μm and undecenoic-acid-treated pSi. For semicarbazide-treated pSi, the proliferation rate was higher compared to glass coverslip until 24 h, and dropped dramatically after 48 h. After 24 h of incubation, the proliferation rate was equivalent on glass coverslip and on flat Si. At 24 h, APTES-treated pSi and semicarbazide-treated pSi improved DPSC proliferation of 27 % and 24 % ($p = 0.042$ and $p = 0.039$, respectively). The proliferation rate was lower on pSi 10 nm, pSi 1 μm and undecenoic acid-treated pSi ($p = 0.012$, $p = 0.004$, and $p = 0.011$, respectively). On pSi 36 nm, this rate was slightly lower compared to glass coverslip and slightly higher compared to pSi 10 nm, but without statistical significance ($p = 0.106$ and $p = 0.094$, respectively). Interestingly, we found that, after 48 and 72 h, the proliferation rate on pSi 36 nm was significantly higher than the rate on pSi 10 nm ($p = 0.006$ at 48 h and $p = 0.003$ at 72 h), revealing the tendency for DPSC to attach and proliferate more on pores of about 36 nm than on pores of about 10 nm. After 72 h of incubation, the proliferation rate was equivalent on flat Si and glass coverslip, higher for 34% on APTES-treated ($p = 0.005$), and lower on pSi 10 nm, and pSi 36 nm.

To confirm the proliferation capacities of DPSC on pSi, we investigated their mitotic activity just after cell seeding, by BrdU incorporation for 24 h. The percentages of BrdU positive cells, corresponding to mitotically active cells, are shown in Figure 5.

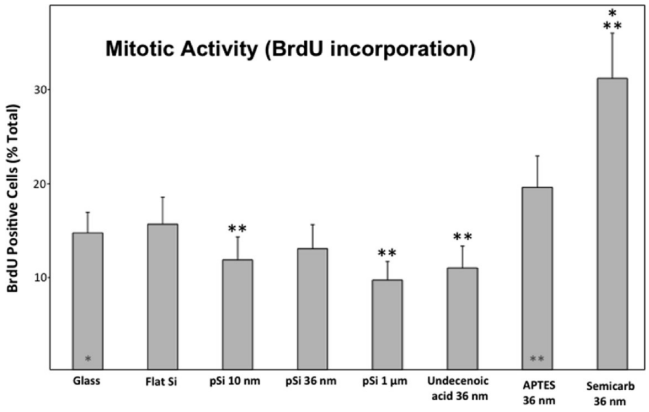

Figure 5. Number of BrdU-positive cells after 24 h of incubation, expressed as a percentage of the total number of DPSCs counted on the various pSi surfaces. Glass coverslip and oxidized nonporous silicon (Flat Si) were used as control. All experiments were performed in triplicate, with a mean number of 60 cells analyzed per sample. Statistical significance was determined by one-way ANOVA Tukey test ($P < 0.05$): (*) comparison with glass coverslip, (**) comparison with APTES.

The ratios of BrdU-positive cells were remarkably enhanced on semicarbazide-treated pSi (29.2 ± 6%) compared to glass coverslip (14.7 ± 4%, $p < 0.001$), Flat Si (15.6 ± 6%, $p < 0.001$), and APTES-treated pSi (19.5 ± 7%, $p = 0.011$). The BrdU-positive cells rate was 14.7 ± 4% on glass coverslip. In comparison, this rate was similar on flat Si (15.6 ± 6%, $p = 0.756$), slightly higher on APTES-treated pSi (19.5 ± 7%, $p = 0.142$), and slightly lower on pSi 10 nm (11.8 ± 5%, $p = 0.331$), on pSi 36 nm (13.0 ± 5%, $p = 0.555$), on pSi 1 μm (9.6 ± 4%, $p = 0.075$) and on undecenoic-acid-treated pSi (10.9 ± 4%, $p = 0.189$).

Cell Morphology. SEM was employed to study the effects of porosity and chemical surface treatments on the morphology of single adhering cells, and to determine cell circularity and cell surface area. Figure 6 shows representative images of DPSC growing on the different pSi substrates and on glass coverslip and flat silicon as controls after 24 h of incubation.

On pSi 10 nm and pSi 36 nm substrates, cells appeared elongated and well-spread with the formation of long protrusions out of the cell membrane (Figure 6C, D). The same shapes were recovered on both glass coverslip and flat Si, even though fewer protrusions were visible (Figure 6A, B). DPSC on APTES-treated and semicarbazide-treated pSi

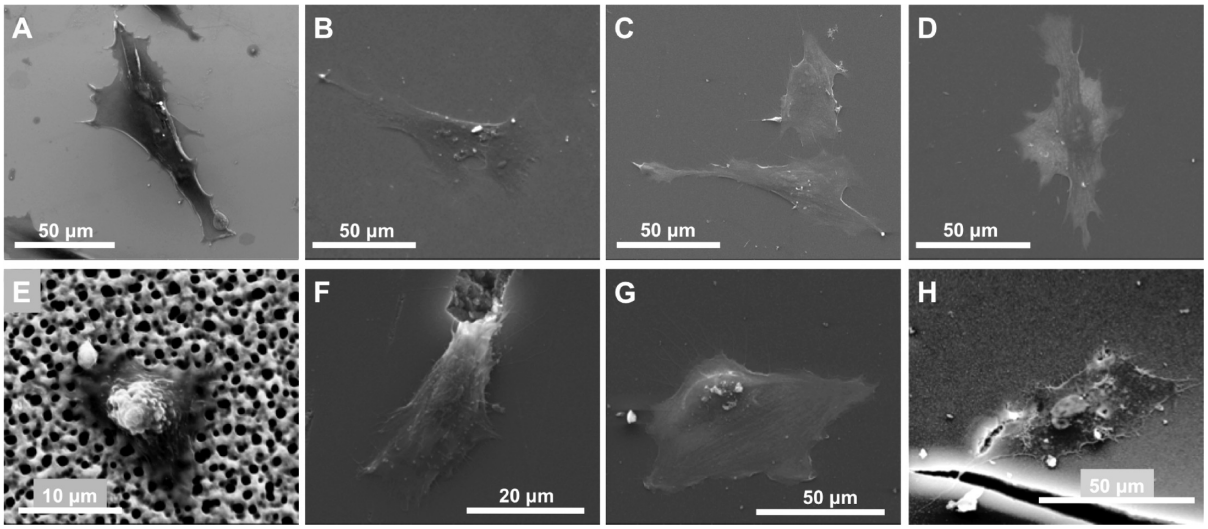

Figure 6. Scanning electron microscopy of DPSC after 24 h incubation. (A) Glass coverslip, (B) flat Si, (C) pSi 10 nm, (D) pSi 36 nm, (E) pSi 1μm, (F) undecenoic acid-treated 36 nm pSi, (G) APTES-treated 36 nm pSi, (H) semicarbazide-treated 36 nm pSi.

appeared less elongated, but well-spread with many long protrusions (Figure 6G, H). Differently, on the pSi 1 μm and undecenoic-acid-treated pSi substrates, cells appeared more rounded with a few short and squat protrusions (Figure 6E, F). Similar images are presented in Figure S1 in the Supporting Information, showing cell protrusions at higher magnification, highlighting the relationship between cells and porous scaffolds at the nanometer scale.

To gain a more quantitative understanding of cell surface adhesion, we determined the cell surface area and circularity on the different substrates (Figure 7).

Compared to glass coverslip, the mean cell surface area was similar on flat Si, pSi 10 nm and semicarbazide-treated pSi; it was higher on pSi 36 nm ($p = 0.040$) and APTES-treated pSi ($p < 0.001$); and it was lower on pSi 1 μm ($p < 0.001$) and undecenoic-acid-treated pSi ($p < 0.001$). APTES-treated pSi had a significantly higher cell surface area compared to all other surfaces (Figure 7A). It is interesting to note that on all surfaces except pSi 1 μm and undecenoic-acid-treated, DPSCs were spread and covered a very large area (between 1290 ± 316 μm^2 on glass coverslip and 1958 ± 314 μm^2 on APTES-treated pSi), which is consistent with the mesenchymal stem cells characteristics.[40] We also considered cell circularity which value varies between 0 (elongated cell) and 1.0 (perfect circle). Comparing directly circularity of cells on the various pSi substrates, morphology was found to vary significantly on three groups of substrates: DPSC had a similar circularity on glass coverslip (0.23 ± 0.06), flat Si (0.22 ± 0.06), pSi 10 nm (0.20 ± 0.07), and pSi 36 nm (0.20 ± 0.05). Cell circularity was similar on APTES-treated (0.34 ± 0.07) and semicarbazide-treated pSi (0.36 ± 0.06), and it was also similar on pSi 1 μm (0.49 ± 0.08) and undecenoic-acid-treated pSi (0.48 ± 0.08) (Figure 7B).

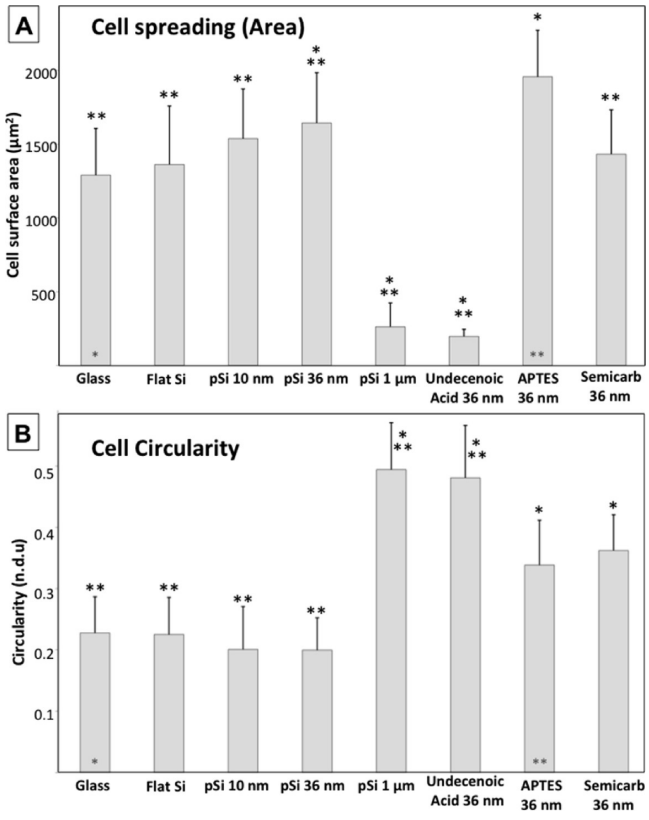

Figure 7. (A) Mean cell surface area calculated from SEM images after 24 h. (B) Mean cell circularity, evaluated from the SEM images 24 h. 0 represents a line and 1.0 a circle (nondefined unitd). A mean number of 25 cells were analyzed per sample. Statistical significance was determined by one-way ANOVA Tukey test ($P < 0.05$): (*) comparison with glass coverslip, (**) comparison with APTES.

Cell Morphology after 72 h. We followed cell growth for 72 h, until they reached confluence on the control surfaces (glass coverslip and flat Si). Cells were stained with the vital dye FDA to observe cell adherence and cytoplasmic spreading. The morphologies of DPSC on surface-modified pSi after 72 h are shown in Figure 8.

As expected according to results presented above, DPSC reached confluence on glass coverslip, flat Si and APTES-treated pSi, growing as clonogenic cell clusters (CFU-F: colony-forming units-fibroblastic) with a high proliferation rate. On pSi 10 nm and pSi 36 nm, DPSC were forming few CFU-F with a moderate proliferation rate, whereas DPSC were hardly growing on pSi 1 μm and undecenoic-acid-treated pSi. The semicarbazide-treated pSi was clearly degraded, with DPSC

dx.doi.org/10.1021/am4046316 | ACS Appl. Mater. Interfaces 2014, 6, 1719−1728

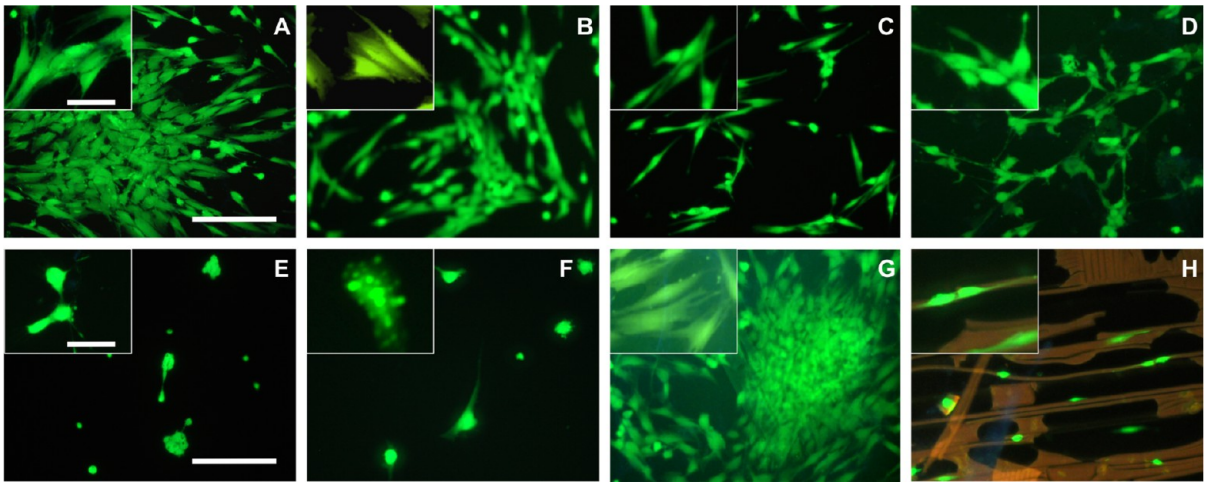

Figure 8. Fluorescence microscopy images of DPSC after 72 h of incubation. Cells are stained with vital FDA. (A) Glass coverslip, (B) flat Si, (C) pSi 10 nm, (D) pSi 36 nm, (E) pSi 1μm, (F) undecenoic acid-treated 36 nm pSi, (G) APTES-treated 36 nm pSi, (H) semicarbazide-treated 36 nm-pSi. Main pictures: ×20, bar = 100 μm. Insets: ×40, bar = 40 μm.

attached only on the porous remaining substrate (Figure 8H), highlighting the fast resorbability of the pSi scaffold.

DISCUSSION

The aim of this work was to elucidate the influence of pore morphology and chemical status of different pSi substrates on immediate human mesenchymal stem cell adhesion and on their proliferation rate. Therefore, we compared the attachment, spreading, morphology, and proliferation of DPSC seeded on different porous surfaces. Our major finding was that pore geometry and surface chemical surface modification strongly influenced the subsequent behavior of DPSC that adhered and proliferated on pSi substrates. It was previously observed that cells could sense nanoscopic features on pSi substrates down to just a few nanometers ($\approx$ 5 nm) and reacted differently to distinctive nanotopographical cues.[4,15,20]

Considering topographical influence, our results showed a higher adhesion and higher proliferation rate for DPSC on pSi substrates with typical pore sizes around 36 nm, as compared to the other pore sizes, at all the considered time points. In term of morphology and spreading, DPSC seemed to react in a similar way on pSi 10 nm and pSi 36 nm as on other substrates such as glass coverslips, and flat Si wafers, with a wider surface area on pSi 36 nm indicating an enhanced cell spreading. On pSi 1 μm, DPSC were not able to proliferate after adhesion and to cover the surface. Even if flat surfaces (glass and flat Si), used as controls in this work, allowed a better cell adhesion compared to porous surfaces, the same proliferation profile was obtained for simple oxidized pSi surface as for the flat surfaces, with the advantage for the porous surfaces to be bioresorbable (Figures 2 and 4). Recently, it has been demonstrated, for four distinct cell types (endothelial cells, mouse fibroblasts, mouse neuroblastoma cells, and human cortical neurons), a higher adhesion on pSi substrates with pore size of 10 nm, as compared to flat silicon or pSi with pore size of 20 nm.[20] Our results clearly portraited a different behavior for human mesenchymal stem cells and confirmed the fact that each cell line had different adhesion characteristics on various pSi surfaces at different time points.[3] As mesenchymal cells, DPSC are involved in structural and fibrous tissues, and their preferential adhesion and proliferation on 36 nm pores could be related to the formation of focal adhesion complex: it has been shown that focal adhesions exhibited a complex multiscale architecture where nanoscopic, doughnut-shaped complexes (~25 nm in diameter and spaced at ~45 nm intervals) were distributed within the adhesion area.[41] More recently, it has been reported that a 34 nm lateral spacing of adhesion peptides increased the formation of mature focal adhesion points.[42] Thus, we hypothesize that DPSC, as other hMSC, have the ability to form mature focal adhesion on pSi with pores around 36 nm, explaining the differences observed in their attachment onto pSi 36 nm, pSi 10 nm, and pSi 1 μm.

After investigating the pore size influence, pSi with 36 nm pores were used to investigate the influence of various surface chemical treatments, including silanization (after thermal oxidation) and hydrosilylation. Hydrosilylation with undecenoic acid offered a limited adhesion and proliferation rate. As already reported in previous works, with other cell types,[3,9] we showed that silanization with APTES encouraged cell attachment, spreading and proliferation, with a significant number of DPSC attached to the pSi surface and a proliferation rate higher than on glass coverslip or flat Si. We also demonstrated here, for the first time, the efficiency of semicarbazide grafted by hydrosilylation for DPSC adhesion and early proliferation. Indeed, semicarbazide-treated pSi permitted cell adhesion, spreading and proliferation similar to those found on APTES-treated pSi, with an even higher rate of mitotically active cells after 24 h. These results are in accordance with studies showing that amine-capped surfaces promoted cell attachment.[43] However, after 48 h, semicarbazide-treated pSi degraded and only few cells remained attached on the surface. In contrast, thermal oxidation, by creating Si−OH bonds at the pSi surface, significantly stabilized pSi in aqueous solution and functionalization with APTES further reduced the rate of hydrolytic dissolution. Thus, the semicarbazide grafting approach on pSi appears not to be used for long-term cell culture in vitro, but offers promising perspectives for cell attraction and immediate transplantation in vivo, as stem cell therapy often requires a scaffold to carry stem cells to the injured site in the body.

CONCLUSION

Here, we have investigated three different pore sizes and three different chemical treatments to evaluate the use of pSi scaffolds for the adhesion and proliferation of primary culture of human

mesenchymal stem cells from the dental pulp. We have identified, for the first time, two efficient amino-grafted pSi scaffolds for human mesenchymal stem cells adhesion and growth, with optimized pore diameter, for in vitro proliferation (and further differentiation), with an interesting potential for in vivo transplantation.

DPSC on pSi 36 nm were observed to have a better adhesion and a faster growth compared to pSi with smaller (10 nm) or larger (1 μm) pore size, in particular after silanization with APTES. Hydrosilylation with semicarbazide led to a new chemical modification favoring cell adhesion and proliferation, especially mitosis after cell adhesion. As this modified pSi surface was stable for only 24−48 h, it appeared to be potentially usable for stem cells adhesion and immediate in vivo transplantation, whereas APTES-treated pSi was more suitable for long term in vitro culture, for stem cells proliferation and differentiation.

More studies are on course to investigate: (1) the ability of APTES-treated pSi as scaffold for stem cells differentiation in different lineage, as pore size might also influence cell differentiation, (2) the optimization of surface stabilization with the semicarbazide treatment, (3) the efficiency of semicarbazide-treated pSi as an immediate cell carrier for in vivo transplantation. Further studies will also elucidate the role played by the porosity on focal adhesion formation, as well as the implication on the cytoskeleton organization.

■ ASSOCIATED CONTENT

Ⓢ Supporting Information

Additional data showing cell protrusions with SEM at high magnification, highlighting the relationship between cells and porous scaffolds at the nanometer scale. Additional images showing water droplets on the various surfaces. This material is available free of charge via the Internet at http://pubs.acs.org.

■ AUTHOR INFORMATION

Corresponding Author

*E-mail: frederic.cuisinier@univ-montp1.fr. Phone: +33 4 11 75 92 52.

Author Contributions

The manuscript was written through contributions of all authors. All authors have given approval to the final version of the manuscript.

Notes

The authors declare no competing financial interest.

■ REFERENCES

(1) Wang, Y.; Kim, H. J.; Vunjak-Novakovic, G.; Kaplan, D. L. *Biomaterials* **2006**, *27*, 6064−6082.
(2) Collart-Dutilleul, P.Y.; Deville de Périère, D.; Cuisinier, F.J.; Gergely, C.; Cunin, F. In *Porous Silicon for Biomedical Applications*; Santos, H., Eds.; Woodhead Publishing: Cambridge, U.K., 2014; Vol. *68*, p 486.
(3) Low, S. P.; Williams, K. A.; Canham, L. T.; Voelcker, N. H. *Biomaterials* **2006**, *27*, 4538−4546.
(4) Khung, Y. L.; Barritt, G.; Voelcker, N. H. *Exp. Cell Res.* **2008**, *314*, 789−800.
(5) Canham, L. T. *Adv. Mater.* **1995**, *7*, 1033−1037.
(6) Ainslie, K. M.; Tao, S. L.; Popat, K. C.; Desai, T. A. *ACS Nano* **2008**, *2*, 1076−1084.
(7) Whitehead, M. A.; Fan, D.; Mukherjee, P.; Akkaraju, G. R.; Canham, L. T.; Coffer, J. L. *Tissue Eng., Part A* **2008**, *14*, 195−206.
(8) Cheng, L.; Anglin, E.; Cunin, F.; Kim, D.; Sailor, M. J.; Falkenstein, I.; Tammewar, A.; Freeman, W. R. *Br. J. Ophthalmol.* **2008**, *92*, 705−711.
(9) Alvarez, S. D.; Derfus, A. M.; Schwartz, M. P.; Bhatia, S. N.; Sailor, M. J. *Biomaterials* **2009**, *30*, 26−34.
(10) Torres-Costa, V. V.; Martínez-Muñoz, G. G.; Sánchez-Vaquero, V. V.; Muñoz-Noval, Á. Á.; González-Méndez, L. L.; Punzón-Quijorna, E. E.; Gallach-Pérez, D. D.; Manso-Silván, M. M.; Climent-Font, A. A.; García-Ruiz, J. P. J.; Martín-Palma, R. J. R. *Int. J. Nanomed.* **2011**, *7*, 623−630.
(11) Park, J.-H.; Gu, L.; von Maltzahn, G.; Ruoslahti, E.; Bhatia, S. N.; Sailor, M. J. *Nat. Mater.* **2009**, *8*, 331−336.
(12) Muñoz Noval, A.; García, R.; Ruiz Casas, D.; Losada Bayo, D.; Sánchez Vaquero, V.; Torres Costa, V.; Martín Palma, R. J.; García, M. A.; García Ruiz, J. P.; Serrano Olmedo, J. J.; Muñoz Negrete, J. F.; del Pozo Guerrero, F.; Manso Silván, M. *Acta Biomater.* **2013**, *9*, 6169−6176.
(13) Noval, A. M.; Vaquero, V. S.; Quijorna, E. P.; Costa, V. T.; Pérez, D. G.; Méndez, L. G.; Montero, I.; Palma, R. J. M.; Font, A. C.; Ruiz, J. P. G.; Silván, M. M. *J. Biomed. Mater. Res. A* **2012**, *100*, 1615−1622.
(14) Dalby, M. J.; Riehle, M. O.; Yarwood, S. J.; Wilkinson, C. D. W.; Curtis, A. S. G. *Exp. Cell Res.* **2003**, *284*, 274−282.
(15) Buxboim, A.; Ivanovska, I. L.; Discher, D. E. *J. Cell Sci.* **2010**, *123*, 297−308.
(16) Sailor, M.J. In *Porous Silicon in Practice: Preparation, Characterization and Applications*; John Wiley & Sons: New York, 2012.
(17) Sapelkin, A. V.; Bayliss, S. C.; Unal, B.; Charalambou, A. *Biomaterials* **2006**, *27*, 842−846.
(18) Wang, P.; Clements, L.; Thissen, H.; Jane, A.; Tsai, W.-B.; Voelcker, N. H. *Adv. Funct. Mater.* **2012**, *22*, 3414−3423.
(19) Clements, L. R.; Wang, P.-Y.; Tsai, W.-B.; Thissen, H.; Voelcker, N. H. *Lab Chip* **2012**, *12*, 1480−1486.
(20) Gentile, F.; La Rocca, R.; Marinaro, G.; Nicastri, A.; Toma, A.; Paonessa, F.; Cojoc, G.; Liberale, C.; Benfenati, F.; di Fabrizio, E.; Decuzzi, P. *ACS Appl. Mater. Interfaces* **2012**, *4*, 2903−2911.
(21) Ma, T. *World J. Stem Cells* **2010**, *2*, 13−17.
(22) Marolt, D.; Knezevic, M.; Novakovic, G. V. *Stem Cell Res. Ther.* **2010**, *1*, 10.
(23) Gronthos, S.; Mankani, M.; Brahim, J.; Robey, P. G.; Shi, S. *Proc. Natl. Acad. Sci. U.S.A.* **2000**, *97*, 13625−13630.
(24) Dominici, M.; Le Blanc, K.; Mueller, I.; Slaper-Cortenbach, I.; Marini, F.; Krause, D.; Deans, R.; Keating, A.; Prockop, D.; Horwitz, E. *Cytotherapy* **2006**, *8*, 315−317.
(25) Coppe, C.; Zhang, Y.; Den Besten, P. K. *Pediatr. Dent.* **2009**, *31*, 467−471.
(26) Shi, S.; Gronthos, S. *J. Bone Miner. Res.* **2003**, *18*, 696−704.
(27) Kémoun, P.; Laurencin-Dalicieux, S.; Rue, J.; Farges, J.-C.; Gennero, I.; Conte-Auriol, F.; Briand-Mesange, F.; Gadelorge, M.; Arzate, H.; Narayanan, A. S.; Brunel, G.; Salles, J.-P. *Cell Tissue Res.* **2007**, *329*, 283−294.
(28) Secret, E.; Smith, K.; Dubljevic, V.; Moore, E.; Macardle, P.; Delalat, B.; Rogers, M.-L.; Johns, T. G.; Durand, J.-O.; Cunin, F.; Voelcker, N. H. *Adv. Healthcare Mater.* **2013**, *2*, 718−727.
(29) Coffinier, Y.; Olivier, C.; Perzyna, A.; Grandidier, B.; Wallart, X.; Durand, J. O.; Melnyk, O.; Stiévenard, D. *Langmuir* **2005**, *21*, 1489−1496.
(30) Tirino, V.; Desiderio, V.; d'Aquino, R.; De Francesco, F.; Pirozzi, G.; Graziano, A.; Galderisi, U.; Cavaliere, C.; De Rosa, A.; Papaccio, G.; Giordano, A. *PLoS ONE* **2008**, *3*, e3469.
(31) Werner, S.; Huck, O.; Frisch, B.; Vautier, D.; Elkaim, R.; Voegel, J.-C.; Brunel, G.; Tenenbaum, H. *Biomaterials* **2009**, *30*, 2291−2301.
(32) Ueda, Y.; Walsh, E.; Nakanishi, H.; Yoshida, K. *Neurosci. Lett.* **1994**, *165*, 203−207.
(33) Horner, P. J.; Power, A. E.; Kempermann, G.; Kuhn, H. G.; Palmer, T. D.; Winkler, J.; Thal, L. J.; Gage, F. H. *J. Neurosci.* **2000**, *20*, 2218−2228.
(34) Cao, D.; Wu, Y.-P.; Fu, Z.-F.; Tian, Y.; Li, C.-J.; Gao, C.-Y.; Chen, Z.-L.; Feng, X.-Z. *Colloids Surf., B* **2011**, *84*, 26−34.

(35) Naveas, N.; Costa, V. T.; Gallach, D.; Hernandez-Montelongo, J.; Palma, R. J. M.; Garcia-Ruiz, J. P.; Manso-Silván, M. *Sci. Technol. Adv. Mater.* **2012**, *13*, 045009.
(36) Jarvis, K. L.; Barnes, T. J.; Prestidge, C. A. *J. Colloid. Interface Sci.* **2011**, *363*, 327−333.
(37) Bateman, J. E.; Eagling, R. D.; Horrocks, B. R.; Houlton, A.; Worrall, D. R. *Chem. Commun.* **1997**, 2275−2276.
(38) Zangooie, S.; Bjorklund, R.; Arwin, H. *J. Electrochem. Soc.* **1997**, *144*, 4027.
(39) Paski, J.; Björkqvist, M.; Salonen, J.; Lehto, V.-P. *Phys. Status Solidi* **2005**, *2*, 3379−3383.
(40) Krishna, O. D.; Jha, A. K.; Jia, X.; Kiick, K. L. *Biomaterials* **2011**, *32*, 6412−6424.
(41) Patla, I.; Volberg, T.; Elad, N.; Hirschfeld-Warneken, V.; Grashoff, C.; Fässler, R.; Spatz, J. P.; Geiger, B.; Medalia, O. *Nat. Cell Biol.* **2010**, *12*, 909−915.
(42) Frith, J. E.; Mills, R. J.; Cooper-White, J. J. *J. Cell Sci.* **2012**, *125*, 317−327.
(43) Faucheux, N.; Schweiss, R.; Lützow, K.; Werner, C.; Groth, T. *Biomaterials* **2004**, *25*, 2721−2730.